Supplementary Information for

Is surface modification effective to stabilize high-voltage cycling for layered P2-$Na_{2/3}Ni_{1/3}Mn_{2/3}O_2$ cathode?

*Fangzhou Niu,[1] Linna Qiao,[2] Heran Huang,[2] Elninoh A. Odero,[1] Guangwen Zhou,[2,3] Hao Liu[1,2]**

[1] Department of Chemistry, Binghamton University, Binghamton, New York 13902, United States

[2] Materials Science and Engineering, Binghamton University, Binghamton, New York 13902, United States

[3] Department of Mechanical Engineering, Binghamton University, Binghamton, New York 13902, United States

*Email: liuh@binghamton.edu

Methods

Synthesis of P2- $Na_{2/3}Ni_{1/3}Mn_{2/3}O_2$: The pristine $Na_{2/3}Ni_{1/3}Mn_{2/3}O_2$ was synthesized by a solid-state method[1]. Stoichiometric amount of $NaNO_3$ (Alfa Aesar), Mn_2O_3 (Sigma-Aldrich) and NiO (Sigma-Aldrich) was ball milled for 30 min to yield a homogeneous mixture. A typical synthesis uses 10 g of the powder mixture. The powder mixture was pressed into a pellet and then calcined at 900 °C in a box furnace for 16 h with a 5 °C/min heating rate. After the furnace was naturally cooled to room temperature, the product was transferred and stored in an Ar-filled glovebox.

Coating of P2- $Na_{2/3}Ni_{1/3}Mn_{2/3}O_2$ with Al_2O_3: Coating of the $Na_{2/3}Ni_{1/3}Mn_{2/3}O_2$ particles was performed following the solution-based method described by Negi et al[2]. A 2 M trimethylaluminum (TMA) solution (Sigma-Aldrich) was diluted into a 0.037 M solution with anhydrous toluene. 5 g of $Na_{2/3}Ni_{1/3}Mn_{2/3}O_2$ powder was added into a 5 mL 0.037 M TMA solution and stirred overnight. Use caution when handling TMA, which is pyrophoric and should be handled with care in dry and inert atmosphere. The powder was washed 3 times with anhydrous toluene and dried at 80 °C overnight in vacuum (denoted as Al-NaNMO-80). The Al_2O_3-coated $Na_{2/3}Ni_{1/3}Mn_{2/3}O_2$ powder was subsequently annealed for 3 h at 300 °C, 400 °C, and 500 °C, which is denoted as Al-NaNMO-300, Al-NaNMO-400, and Al-NaNMO-500, respectively.

Electrode Fabrication: The composite electrode is consisted of the active material, carbon black, and polyvinylidene difluoride (PVDF) in 8:1:1 weight ratio. 200 mg of active material was used in a typical electrode preparation. Stoichiometric amount of active material and carbon black was mixed for 10 minutes using mortar and pestle. Stoichiometric PVDF gel (10% w/w in N-methylpyrrolidone solvent, NMP) was added into the powder mixture. Additional NMP solvent (typically 0.2 mL for 200 mg of active material) was introduced to achieve the desired viscosity of the slurry. Thinky mixer AR-100 was used to mix the slurry at 2000 rpm for 30 minutes. The slurry was cast on an Al foil using a doctor blade with a 150 μm gap. The film was dried at 120 ℃ in vacuum overnight. The electrodes were cut to disks of 10 mm in diameter and stored in an Ar-filled glovebox. The typical areal mass loading is 3.8 mg/cm^2.

Galvanostatic cycling: CR2032 cells were assembled with sodium metal as the anode, $Na_{2/3}Ni_{1/3}Mn_{2/3}O_2$ as the cathode, glass fiber as the separator, and 1 M $NaClO_4$ in propylene carbonate (PC) with 2% (v/v) fluoroethylene carbonate additive as the electrolyte. The galvanostatic charge and discharge tests were performed for the pristine and the Al2O3-coated electrodes at C/20 (1 C = 260 mAh/g) between 2 V and 4.5 V. The cycling test was conducted by a LAND cycler.

Electrochemical Impedance Spectroscopy (EIS): EIS was measured in CR2023 half cells for both the pristine and Al-NaNMO-400 electrodes with a BioLogic BCS-805 cycler. Cells were initially charged 4.5 V at C/20 with the EIS performed at 3.75V on discharge. Subsequent cycling was only performed within the voltage window of 3.75 – 4.5 V, where the EIS was conducted at the end of discharge at 3.75 V. Before each EIS measurement, the cell was held at 3.75 V until the current decreased to C/100 to reach the equilibrium state. The frequency range spans from 100 kHz to 0.01 Hz with an AC voltage amplitude of 10 mV.

Materials Characterization: X-ray powder diffraction (XRD) was conducted with a Bruker D8 Advance X-ray diffractometer using Mo Kα (0.71 Å) radiation in Bragg-Brentano geometry. The 2θ range was from 5.5° to 55°. Rietveld refinement was performed using GSAS-II[3].

Operando XRD was performed for the pristine and Al-NaNMO-400 electrodes in customized coin cells with the same diffractometer in transmission geometry. CR2016 cells with rectangular slits (10 mm × 2 mm) were used to allow transmission of X-ray through the cell (Figure S10). The coin cells were cycled with a BioLogic BCS-805 cycler from 3.75 V to 4.5 V at C/10. Sequential Pawley fitting was conducted using TOPAS Academic v6[4]. An anisotropic microstrain broadening model was used to fit the peak broadening of both the P2 and O2 phases. The sample microstrain broadening was described by $\beta_{hkl} = e_{hkl} \tan\theta$, where β_{hkl} and e_{hkl} correspond to the *hkl*-dependent full width at half maximum and the refined microstrain parameter, respectively. e_{hkl} is defined and refined independently for (*h*00), (00*l*) and all other reflections to account for the anisotropic peak broadening.

X-ray photoelectron spectroscopy (XPS) was performed with PHI 5000 using an Al anode source at 1.5 KeV. For each sample, survey scans were collected in 1.0 eV increments, followed by high-resolution scans with a step size of 0.05 eV for C 1s, Al 2p, and Ni 3p. The binding energy was calibrated using adventitious carbon, with the C-C peak set to 284.8 eV.

High-resolution Transmission Electron Microscopy (HRTEM) analysis was conducted using a JEOL JEM 2100F TEM operating at 200 kV for both pristine and Al-NaNMO-80 samples. Given the trace amount of Al on the surface of NaNMO, elemental distribution in Al-NaNMO samples was examined using FEI Talos 200X scanning TEM operated at an accelerating voltage of 200 kV. This instrument offers superior sensitivity in dispersive X-ray spectroscopy (EDS) analysis, in addition to high-angle annular dark-field (HAADF) imaging.

Elemental Analysis was performed using a VISTA-MPX instrument employing inductively coupled plasma-optical emission spectroscopy (ICP-OES).

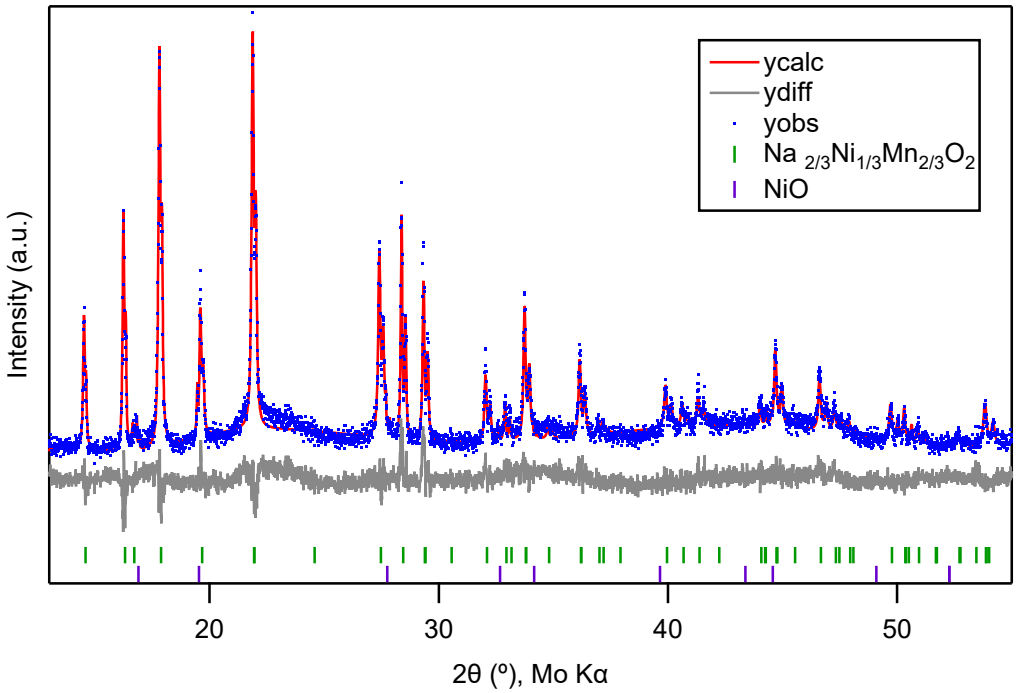

Figure S1. Fitting profile for the Rietveld refinement of the pristine $Na_{2/3}Ni_{1/3}Mn_{2/3}O_2$ sample.

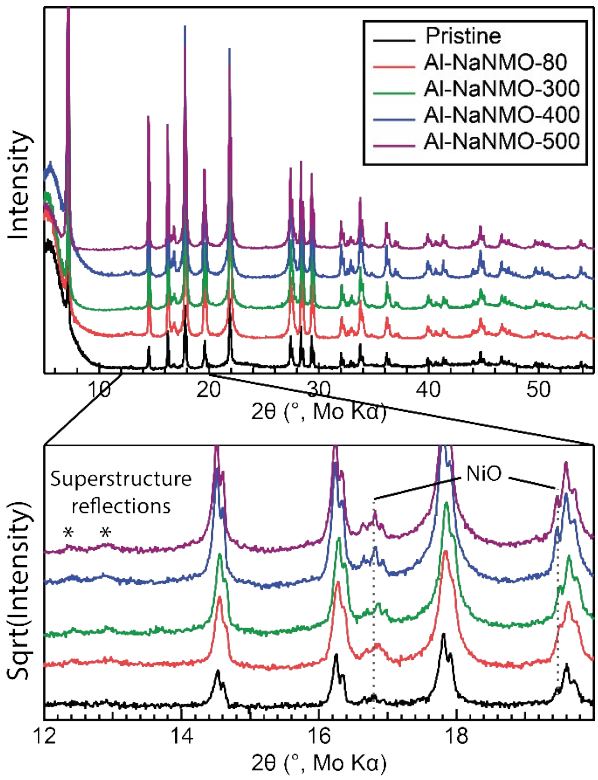

Figure S2. X-ray powder diffraction patterns measured for the pristine $Na_{2/3}Ni_{1/3}Mn_{2/3}O_2$ and the TMA-treated $Na_{2/3}Ni_{1/3}Mn_{2/3}O_2$ dried at 80 °C (Al-NaNMO-80) and annealed at 300 °C (Al-NaNMO-300), 400 °C (Al-NaNMO-400), and 500 °C (Al-NaNMO-500). Superstructure reflections are indicated by asterisks. Peaks corresponding to the NiO impurity phase are indicated by dashed grey lines.

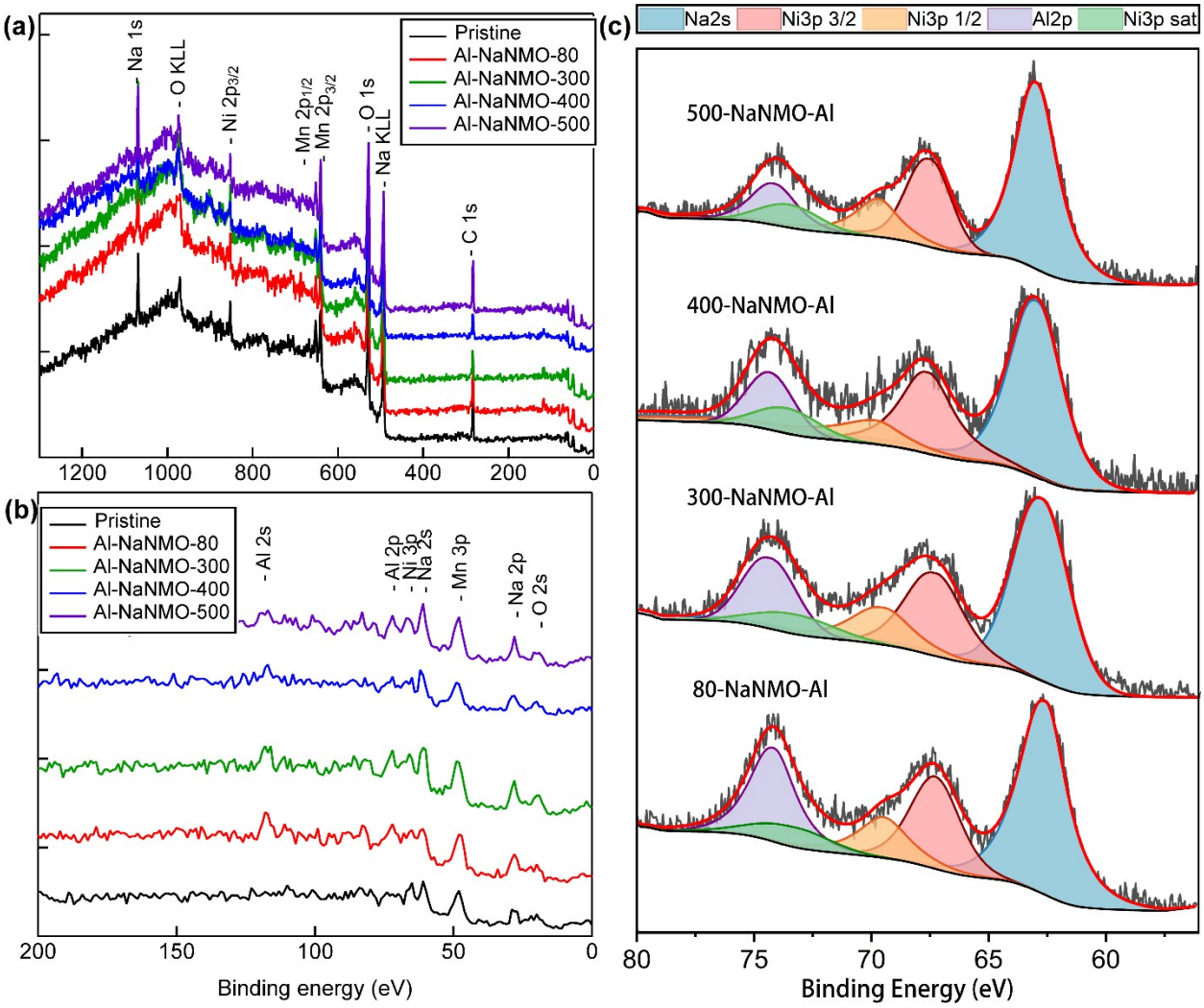

Figure S3. X-ray photoelectron spectroscopy measured for the Al-NaNMO-80, Al-NaNMO-300, Al-NaNMO-400, and Al-NaNMO-500 samples. (a-b) Survey scan between 1200 and 0 eV. (c) High-resolution spectra between 80 and 52 eV. The red curve corresponds to the fitting profile with the contributing peaks shown with solid color fills.

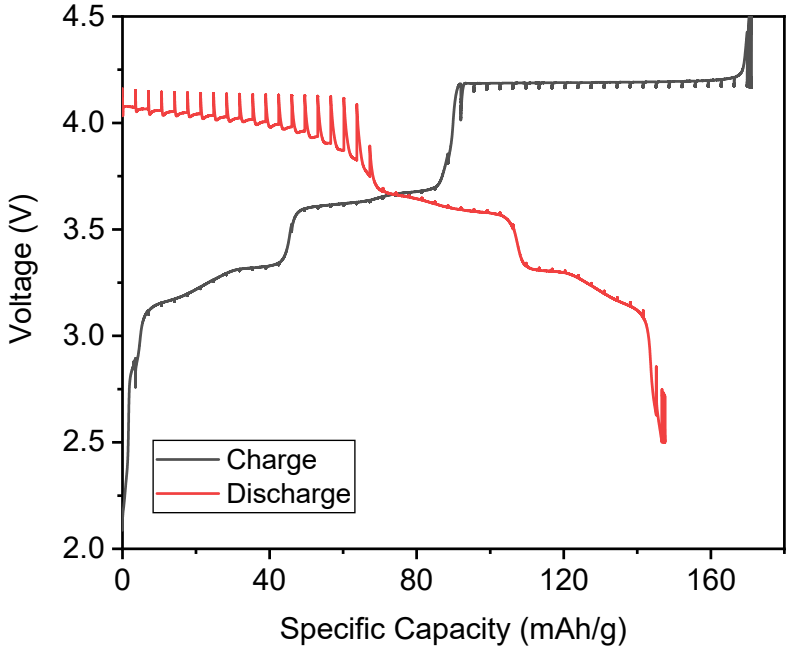

Figure S4. Voltage profile vs specific capacity measured by the galvanostatic intermittent titration technique (GITT) for first charge and discharge of the pristine $Na_{2/3}Ni_{1/3}Mn_{2/3}O_2$ electrode.

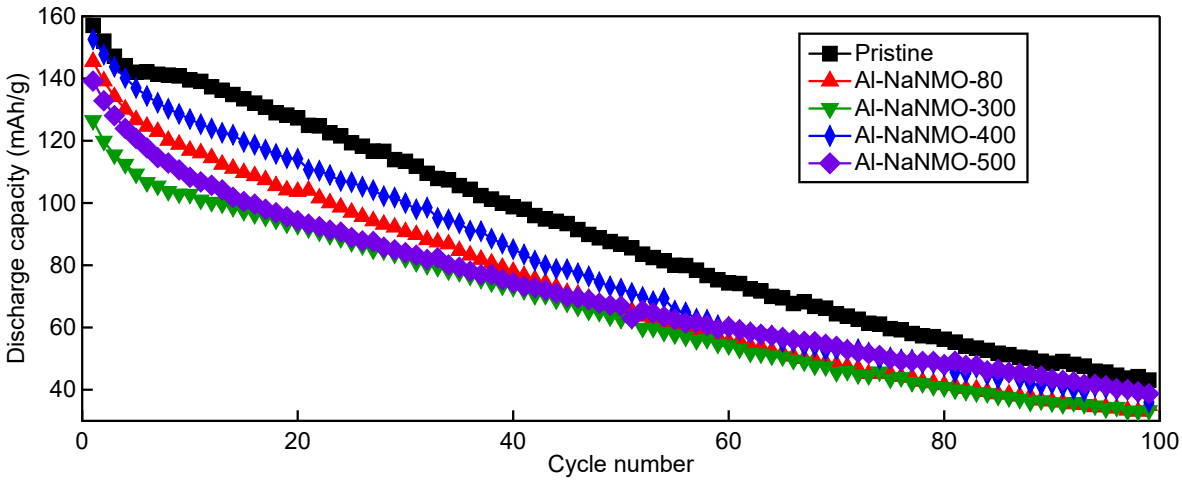

Figure S5. Specific discharge capacity for the pristine and surface-modifed samples cycled between 2.5 V and 4.5 V at C/20 (1 C = 260 mA/g).

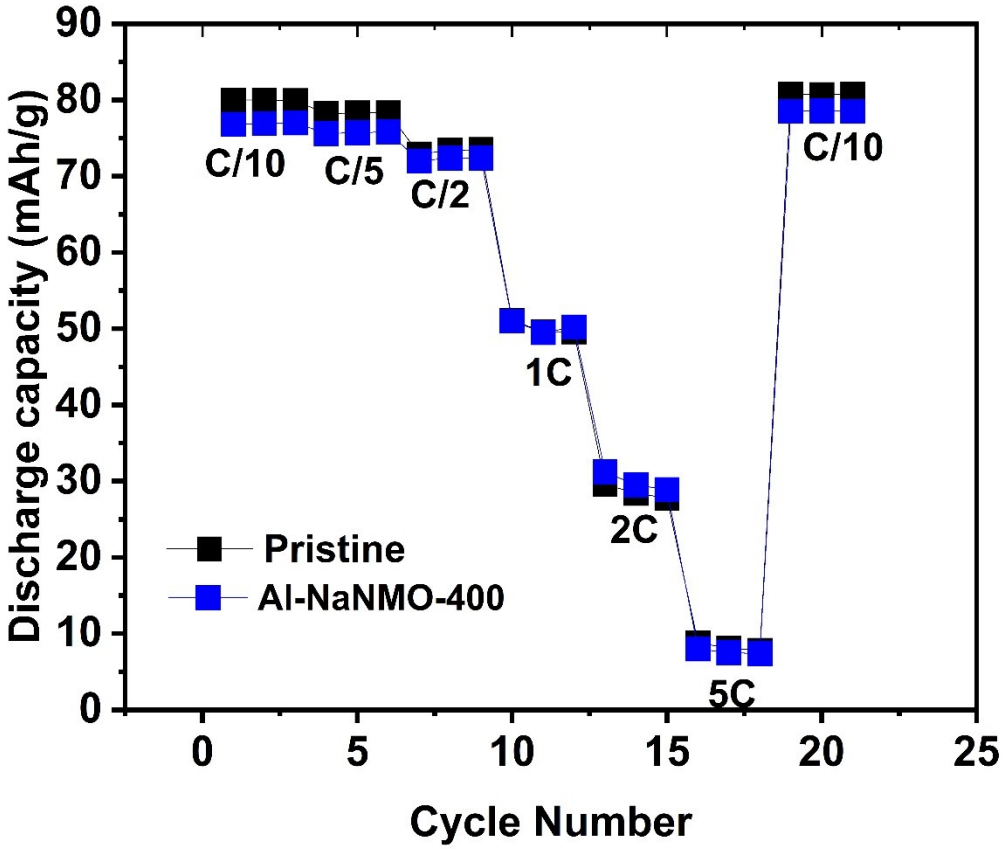

Figure S6. Specific discharge capacity measured in the voltage window of 2.5 – 4.0 V for the pristine and Al-NaNMO-400 electrodes at different charging and discharging rates.

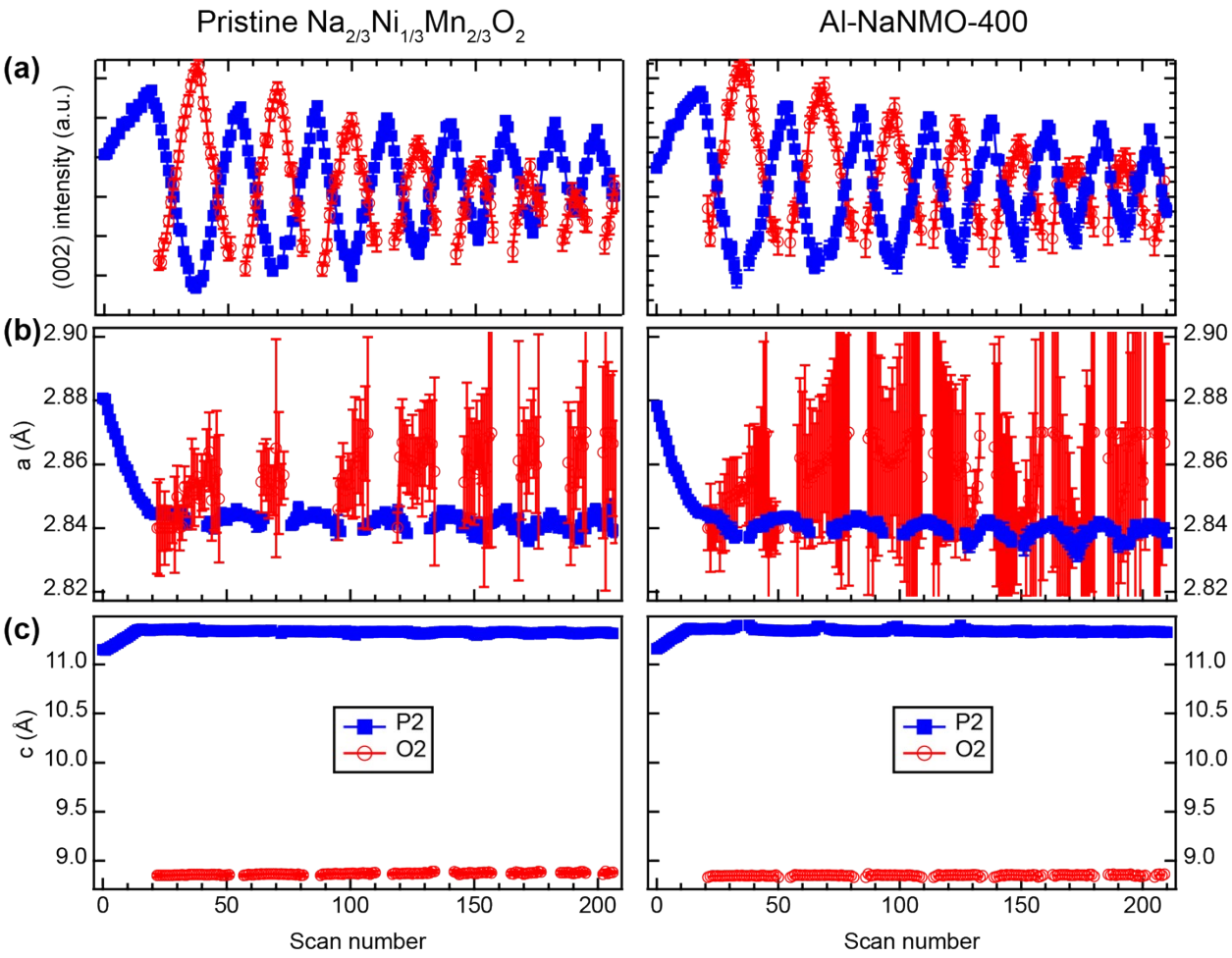

Figure S7. Pawley fitting results for the operando XRD data. (a) Integrated intensity of the (002) reflection for both the P2 and O2 phases. (b) *a* and (c) *c* unit cell parameters for both the P2 and O2 phases.

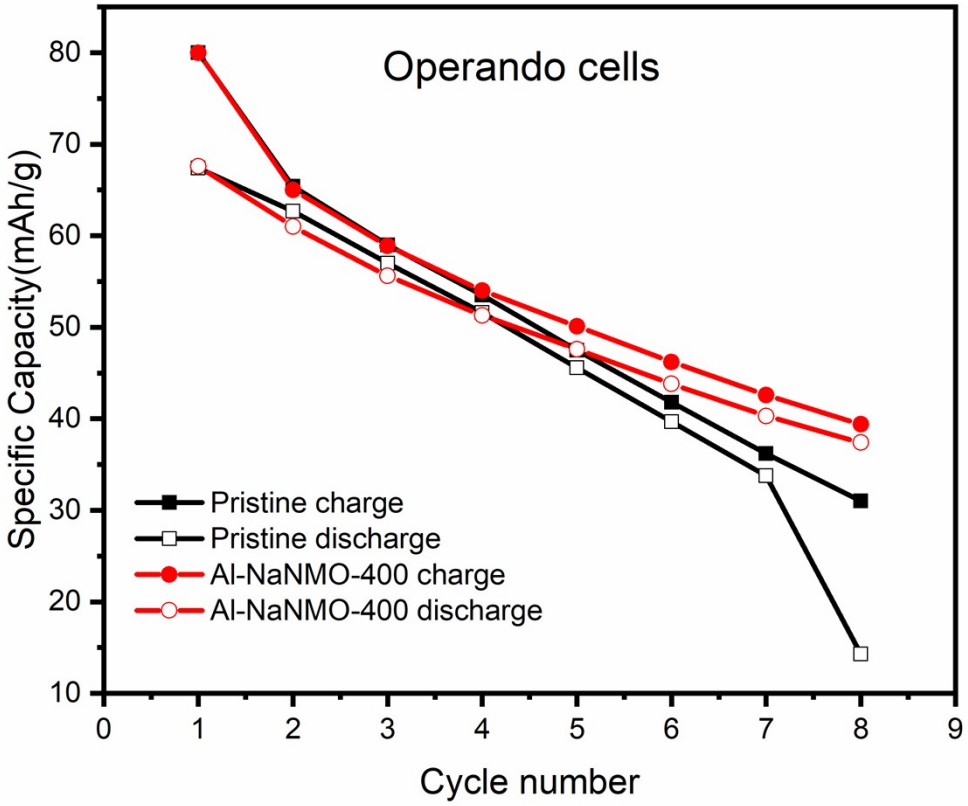

Figure S8. Specific capacity of the operando cells cycled in the voltage window of 3.75 – 4.5 V at C/20 (13 mAh/g) for both the pristine and Al-NaNMO-400 electrodes.

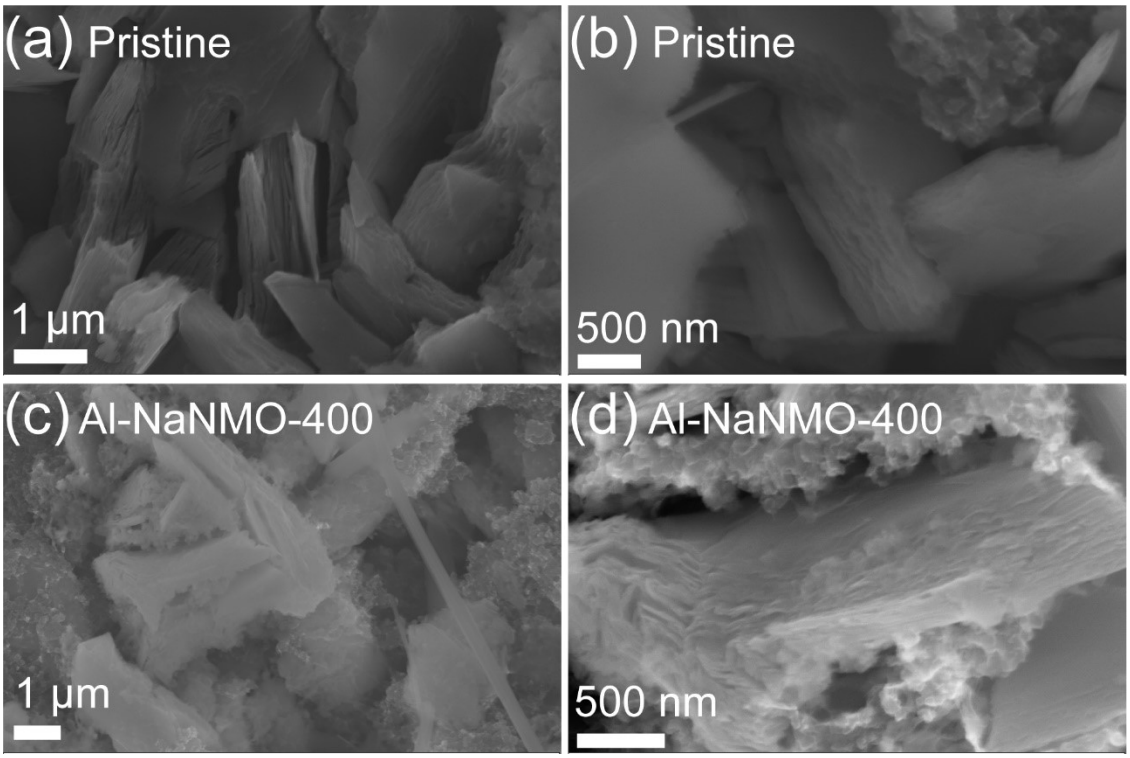

Figure S9. SEM images of the (a and b) pristine and (c and d) Al-NaNMO-400 electrode samples harvested after 99 charge-discharge cycles between 2.5 V and 4.5 V at C/20 (1 C = 200 mA/g). Significant cracking, kinking, and delamination are found in both samples.

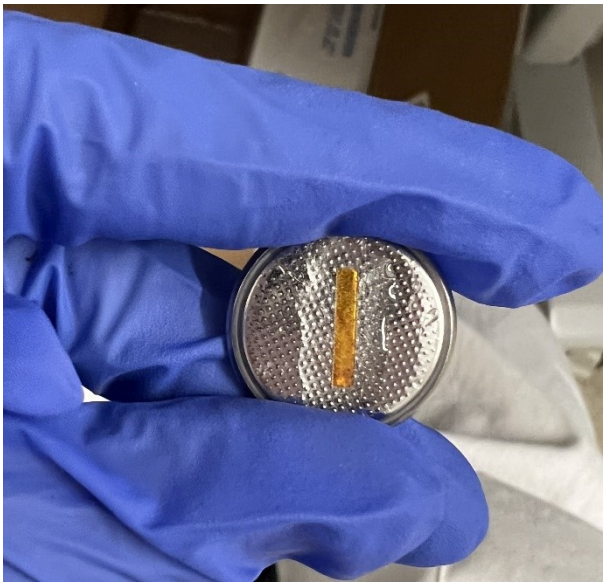

Figure S10. Photograph of the customized CR2016 cell used for the operando XRD measurement in transmission geometry. A rectangular slit (10 mm × 2 mm) was cut on both the top and bottom cases to allow for the transmission of the X-ray. The slit was sealed by a Kapton film from the inside and epoxy glue from the outside of the cell case.

Table S1. Rietveld refined unit cell parameters and phase fraction for the pristine, Al-NaNMO-80, Al-NaNMO-300, Al-NaNMO-400 and Al-NaNMO-500 samples.

Sample	**NiO wt%**	**a (Å)**	**c (Å)**	**Volume (Å^3)**
Pristine	1.8(1)	2.8873(1)	11.1733(7)	80.669(9)
Al-NaNMO-80	1.83(6)	2.8878(1)	11.1754(7)	80.71(1)
Al-NaNMO-300	1.82(6)	2.8868(1)	11.1796(7)	80.684(8)
Al-NaNMO-400	1.88(5)	2.8874(1)	11.1774(5)	80.705(7)
Al-NaNMO-500	1.84(6)	2.8874(1)	11.1782(6)	80.706(8)

Table S2. Elemental analysis results for the pristine and Al-NaNMO-400 samples.

Elements	Ni	Mn	Na	Al
Pristine (ICP)	33.7%	66.3%	79.3%	-
Al-NaNMO-400 (HADFF-EDS mapping)	32.7%	67.3%	37.4%	0.7%

Table S3. XPS fitting results of Al region for the Al-NaNMO-80, Al-NaNMO-300, Al-NaNMO-400 and Al-NaNMO-500 samples.

	Al-NaNMO-80		Al-NaNMO-300		Al-NaNMO-400		Al-NaNMO-500	
Component	Binding Energy (eV)	Area CPS.eV	Binding Energy (eV)	Area CPS.eV	Binding Energy (eV)	Area CPS.eV	Binding Energy (eV)	Area CPS.eV
Na2s	62.48	600.57	62.83	655.98	62.85	328.35	62.95	568.70
Ni3p 3/2	67.19	282.21	67.32	291.68	67.50	147.81	67.51	280.21
Ni3p 1/2	69.39	141.10	69.52	145.85	69.70	73.90	69.71	140.11
Ni3p sat	73.19	87.48	73.32	90.42	73.50	45.82	73.51	86.86
Al2p	74.08	268.02	74.31	221.00	74.26	79.15	74.15	127.35
Al2p :(Ni3p 3/2 +Ni3p 1/2)	0.63		0.51		0.36		0.30	

Table S4. Constraints used in the XPS fitting of the Al2p spectrum region.

Component	Binding Energy (eV)	FWHM	Area constraints
Na2s	62.0-63.0	2:04	
Ni3p 3/2	66.0-67.5	2:04	
Al2p	72.0-75.0	1:03	
Ni3p 1/2	C+2.2	C*1.0	C*0.5
Ni3p sat	C+6.0	3:05	C*0.31

References

1 G. Singh, N. Tapia-Ruiz, J. M. Lopez Del Amo, U. Maitra, J. W. Somerville, A. R. Armstrong, J. Martinez De Ilarduya, T. Rojo and P. G. Bruce, *Chemistry of Materials*, 2016, **28**, 5087–5094.

2 R. S. Negi, S. P. Culver, A. Mazilkin, T. Brezesinski and M. T. Elm, *ACS Appl Mater Interfaces*, 2020, **12**, 31392–31400.

3 B. H. Toby and R. B. Von Dreele, *J Appl Crystallogr*, 2013, **46**, 544–549.

4 A. A. Coelho, *J Appl Crystallogr*, 2018, **51**, 210–218.